Colloid Polym Sci (2005) 283: 359–366
DOI 10.1007/s00396-004-1146-8

ORIGINAL CONTRIBUTION

Hideya Kawasaki
Masaaki Shinoda
Masahiko Miyahara
Hiroshi Maeda

Reversible pH-induced transformation of micellar aggregates between hemicylinders and laterally homogeneous layers at graphite-solution interfaces

Received: 19 January 2004
Accepted: 16 April 2004
Published online: 25 May 2004

H. Kawasaki (✉) · M. Shinoda
M. Miyahara · H. Maeda
Department of Chemistry,
Faculty of Science, Kyushu University,
33 Hakozaki, Higashi-ku,
812–8581 Fukuoka, Japan
E-mail:
hkawascc@mbox.nc.kyushu-u.ac.jp
Tel.: +81-92-6424367
Fax: +81-92-6422607

Abstract pH-induced transformation between a hemicylindrical aggregate and a laterally homogeneous layer at the graphite-solution interface was demonstrated in micellar aggregates of dodecyldimethylamine oxide (C12DMAO) using atomic force microscopy (AFM). Nonionic C12DMAO (pH∼8) and fully-ionized cationic C12DMAO (pH∼1.5) both formed hemicylindrical aggregates on graphite, similar to aggregates formed by many other ionic (or nonionic) surfactants on graphite. However, a laterally homogeneous layer was observed in the case of nearly half-ionized C12DMAO around pH∼4 (a 1:1 mixture of the nonionic and the cationic species). These results indicated that the surface curvature of the C12DMAO aggregates on graphite was the smallest around the degree of ionization $\alpha = 0.5$, despite charging up the nonionic hemicylindrical aggregates. Using AFM images and the corresponding force curves, the transformation between the hemicylindrical aggregate and the laterally homogeneous layer was found to be reversible via a change in pH. The formation of the laterally homogeneous layer of nearly half-ionized C12DMAO is explained by hydrogen bond formation between the nonionic and the cationic headgroups.

Keywords Hemimicelle · Graphite/solution interface · AFM · pH-induced transformation · Amine oxide surfactants

Introduction

Surfactants spontaneously aggregate to form microstructures (hemimicelles) at solid-solution interfaces in a manner analogous to micellization in bulk solution. The existence of these hemimicelles was first proposed by Fuerstenau in 1955 [1, 2]. Recently, Atomic Force Microscopy (AFM) has provided a new insight into the structures of the micellar aggregates at solid-solution interfaces [3, 4, 5]. Reviews of the micellar aggregates at solid/solution interfaces are given in [6, 7]. Manne et al [3] and Ducker et al [5] demonstrated the direct observation of hemimicelles at the graphite(crystalline hydrophobic surface)-solution interface by means of AFM. The AFM studies indicated that the dominant aggregate structures at the graphite-solution interface were hemicylinders. Cationic, anionic, zwitterionic and nonionic surfactants with alkyl chains of twelve carbons or more all form hemicylindrical aggregates on graphite [5, 6, 7, 8, 9, 10, 11], in contrast to micellar aggregates at mica-solution interfaces [6, 7, 8]. It has been reported that the graphite surface templates the formation of hemicylindrical aggregates due to a good fit between the surfactant alkylchain length and the graphite lattice [3, 12, 13]. The horizontal adsorbed monolayer on the graphite surface has a head-to-head and tail-to-tail arrangement, which templates further adsorption and finally leads to the hemicylindrical aggregate on the

graphite. This process is supported by a thermodynamic analysis of calorimetric enthalpies and adsorption isotherms [13]. It is known that the surfactants generally have a minimum required surfactant tail length (typically dodecyl group length) to self-assemble as hemicylinders on graphite; below the dodecyl group length they form a laterally homogeneous layer on graphite [6, 7, 12]. As is the case for relatively smooth amorphous hydrophobic surfaces, several surfactants formed globular structures [15] or laterally unstructured layers [12, 14] at the hydrophobic solid-solution interface. In addition to the AFM studies, hemicylindrical aggregates at the graphite-solution interface have been studied by theoretical modeling [16, 17]. The AFM studies mentioned above show that the micellar aggregates at the graphite-solution interface are hemicylinders or laterally homogeneous layers. As yet, there have been no reports about the reversible structural transitions of the micellar aggregates at the graphite-solution interface, between the hemicylinder and the laterally homogeneous layer.

Alkyldimethylamine oxide (CnDMAO) solutions are mixtures of the nonionic [$C_nH_{2n+1}(CH_3)_2N \rightarrow O$] and the ionized (protonated) cationic species [$C_nH_{2n+1}(CH_3)_2N^+OH$]. The composition α_m (the degree of ionization) of the micelle is determined by the pH for a given ionic strength. It has been reported that mixtures of the protonated and the unprotonated species show an extremely strong synergism in micellar solutions as well as the solid state [18, 19, 20, 21, 22, 23, 24, 25, 26, 27, 28, 29, 30], which may originate from hydrogen bonds between the cationic and nonionic headgroups (-N^+-OH··O-N-) [24, 25, 28]. Here, we are concerned with how the protonation in the CnDMAO surfactant system affects the aggregate structures at the solid-solution interface. In a previous paper, we reported the effect of ionization (pH) on the aggregate structures of tetradecyldimethylamine oxide (C14DMAO) surfactants at the graphite-solution interface, as well as at the mica-solution interface, via AFM [31]. At the mica-solution interface, C14DMAO formed aggregates with decreasing curvature as the degree of ionization of C14DMAO was increased. Nonionic C14DMAO formed short cylindrical aggregates on mica, while flat bilayers on mica were observed for the half-ionized C14DMAO and the fully ionized C14DMAO. The formation of flat bilayers emphasizes the higher packing parameter character of the C14DMAO surfactant, compared to the cationic quaternary ammonium surfactant with a single tetradecyl tail, which forms the cylindrical aggregate on mica [8]. The suggested reason for this lower curvature of the C14DMAO aggregate was the hydrogen bonds between the headgroups in the flat bilayer. Contrary to the micellar aggregates on mica, the dominant structures of C14DMAO on graphite were hemicylinders, irrespective of the ionization. The ionization increased the distances between the hemicylindrical aggregates due to the electrostatic repulsion between the aggregates, rather than inducing a change in the aggregate structure. The weak dependence of the aggregate structures on the ionization was suggested to be due to the dominant attractive interaction between the graphite surface and the tetradecyl group.

In this work, we investigated the effect of protonation on the aggregate structures of dodecyldimethyl amine oxide (C12DMAO) surfactants at graphite-solution interfaces via AFM. Compared to the case of C14DMAO, the attractive interaction between the dodecyl group of C12DMAO and the graphite surface is weaker due to the shorter surfactant tail. As a result, the interaction between the headgroups would be the main factor in determining the shape of the C12DMAO aggregate on graphite. In the present study, we show the pH-induced transformation of the micellar aggregates between the hemicylinder and the laterally homogeneous layer at the graphite-solution interface. The reversibility of the pH-induced transformation is also examined by the AFM images and the corresponding force curves.

Experimental

Sample preparation

Water was prepared by distillation and then passed through an ultrapure water system consisting of an ion exchange, an activated carbon cartridge, and a 0.2 μm filter (Branstead Co.). The resulting water has a conductivity of 18 $M\Omega^{-1}$ cm^{-1} at 25 °C. Dodecyldimethylammine oxide (C12DMAO) (Gerbu Co.) was recrystallized three times from hot acetone. After recrystallization, there was a single peak in the high performance liquid chromatography (HPLC) chromatograms produced by a ODS-120T (Tosoh Co., Japan) column ($MeOH/H_2O = 7/3$). Oleydimethylamine oxide (OleyDMAO) was obtained from oleyldimethylamine (Lion Ako) via oxidation in ethanol by hydrogen peroxide following, in most part, the procedure similar to that used for other alkyldimethylamine oxides, and purified by the extraction of the unreacted amine by hexane [30].

The degree of ionization for the C12DMAO aggregates on the solid at a given pH in the present study is not clear. However, we defined that the degree of ionization at the interface is that of the micelle in bulk solution α [31], although there may be some difference in composition between the surface aggregates and the bulk micelles [32]. The intrinsic proton dissociation constant of the amine oxide micelle, p K_M, is 5.9 for C12DAO spherical micelles and 6.3 for C14DAO rodlike micelles [25, 33]. For the oleydimetylamine oxide surfactant, the electric surface properties of the worm-

like micelles and the vesicles are found to be very similar, despite a large difference in shape between them [34]. Therefore, in the case of the C12DMAO, there may a small difference in the ionizations (at a given pH) between the bulk spherical micelle and the hemicylindrical aggregates on graphite due to slightly different curvatures between the two kinds of aggregates. The pH values of the solutions were adjusted using HCl or NaOH.

Microscopy

AFM images were captured with a SPA 400 (Seiko Instruments Co., JAPAN) instrument, using silicon nitride tips (OLYMPUS Co., JAPAN) with a nominal spring constant of 0.09 N m^{-1} and a fluid cell. Crystalline graphite was glued to the microscope slides using epoxy glue of a low melting temperature, and then freshly cleaved with adhesive tape in laminar flow. Prior to use, the cantilevers were irradiated in laminar flow with ultraviolet light (8 mW cm^{-2} at 253.7 nm) for about 20 min and then washed with distilled ethanol. The surfactant was adsorbed onto the surface of the freshly cleaved graphite by immersing the substrate in the surfactant solutions of desired composition for at least 24 h. AFM imagings were performed for the substrates in the surfactant solutions at 25 ± 2 °C. Deflection images (showing the error in the feedback signal) were collected with scan rates of 5–10 Hz. No filtering of images was performed other than that inherent in the feedback loop. Zero distance in the force curves is where a constant high gradient of force is measured and it is assumed to be where the tip is touching the substrates. AFM imagings were performed at a repulsive force from the adsorbed films with the tip separated from the substrates by about 1–3 nm (so called *soft contact imaging*) [35].

Results and discussion

The pH-induced morphological changes of the micellar aggregates of C12DMAO on graphite

Figure 1 shows the AFM images of the micellar aggregates on graphite for nonionic C12DMAO ($\alpha = 0$, pH 8.0 ± 0.1) and cationic C12DMAO ($\alpha = 1$, pH 1.3 ± 0.1). The surfactant concentration was fixed to be about twice of the bulk critical micellar concentration (cmc). The AFM images at $\alpha = 0$ and at $\alpha = 1$ both show parallel stripe structures, suggesting the formation of hemicylindrical aggregates. The formation of hemicylindrical aggregates on graphite for both nonionic and cationic C12DMAO is in general agreement with reported observations for many other ionic and nonionic surfactants where the surfactant tail is longer than a decyl group, which also formed hemicylindrical aggregates on graphite [5, 8, 9, 10, 11].

To see the ionization effect on the aggregate structures of C12DMAO at the graphite-solution interface, we examined the aggregate structures at various α values (pH values). Figure 2 shows the AFM images at $\alpha = 0.05$, 0.15, 0.25, 0.37, 0.47, 0.55, 0.8, and 0.9 in the surfactant solutions of about twice cmc. The hemicylindrical aggregates are formed at the graphite-solution interface below $\alpha = 0.25$ (Figs. 2a,b,c). As the ionization increases from $\alpha = 0.25$–0.37, the aggregate structure on graphite changes from the hemicylindrical aggregate (Fig. 2c) to a laterally homogeneous layer (Fig. 2d). Increasing the ionization further induces another transformation, from the laterally homogeneous layer at $\alpha = 0.47$ (Fig. 2e) back to the hemicylindrical aggregates above $\alpha = 0.55$ (Figs. 2f,g,h). These pH-induced morphological changes of the C12DMAO aggregate take place over a narrow range of pH: hemicylinder (pH≥5), to laterally homogeneous layer ($4.5 \geqq pH \geqq 4$), to hemi-

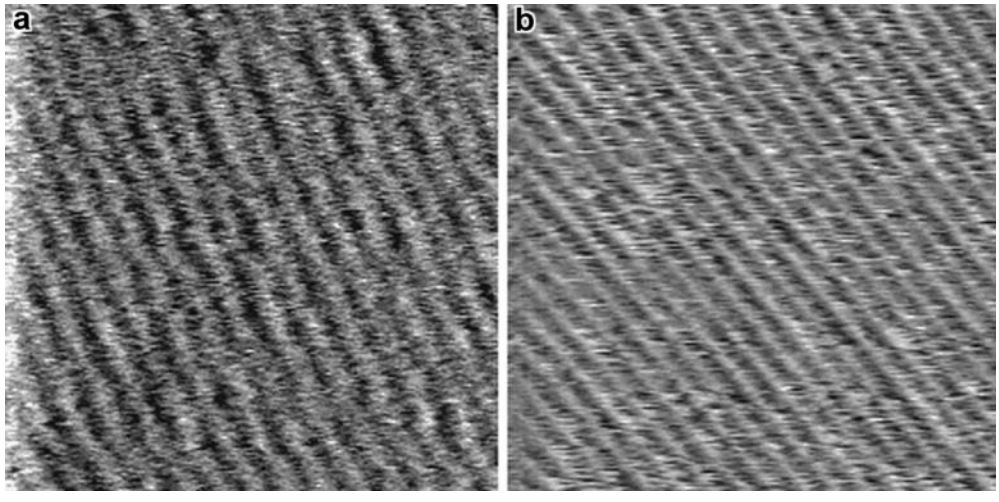

Fig. 1a–b AFM images showing the aggregate structure of nonionic C12DMAQ and cationic C12DMAO at the graphite-solution interface (100× 100 nm^2). The surfactant concentration C_d was fixed to be about twice cmc. **a** $\alpha = 0$, pH 8.0 ± 0.1, $C_d = 3$ mM; **b** $\alpha = 1$, pH 1.3 ± 0.1, $C_d =$ 10 mM

cylinder (pH $\leqq$ 3.7). The above results show the pH-induced transformation of the micellar aggregate of C12DMAO on graphite between the hemicylinder and the laterally homogeneous layer, in contrast to the behavior of C14DMAO [31]. It would be interesting to know how the structures of the C12DMAO aggregate transform between the hemicylinder and the laterally homogeneous layer upon changing pH, but since our AFM images were from tip deflection mode [5, 9], and the change in measured height across an aggregate during imaging was typically about 0.1–0.2 nm, they could not give a detailed picture of the cross-section of the adsorbed aggregate on graphite. However, the AFM images do reveal the repeat unit, or the period of the aggregate structures. Therefore, we focused upon the pH dependence of the periodic structure of the hemicylindrical aggregates in this study. It has been suggested that the period of the structure of the hemicylindrical aggregates is equal to the diameter of a hemicylindrical aggregate plus the intermicellar distance (*ND*) [5, 9], as shown in Fig. 3. The *ND* values can be obtained from a clear maximum in the period of the Fourier transform of the AFM image. Figure 3 shows the ionization dependence of the *ND* values for the hemicylindrical aggregate of C12DMAO. Except for $\alpha = 1$, the ND values are weakly dependent on the α value within the experimental error, and they are 5 ± 0.5 nm. The *ND* values are about twice the length of a C12DMAO molecule ($\sim$2 nm), which is consistent with the length expected from the hemicylindrical structure. The *ND* value at $\alpha = 1$ is the most smallest, which may be partially due to the high ionic strength of the solution at $\alpha = 1$ (the lowest pH value is $\sim$1.3), leading to the screening of the electrostatic forces between the hemicylindrical aggregates (in other words to a decrease in the *ND* value). The result that remains unexplained is the observation that the *ND* values are weakly dependent on the α values. The lack of dependence on the ionization implies either that the repulsive electrostatic forces are not strong enough, or that another effect cancels out this contribution (such as a change in the diameter of the hemicylindrical aggregate). There may be some difference in the degree of ionization between the surface aggregates and the bulk micelles, or the effective surface charge density of the surface aggregate may be weakly dependent on the α values due to significant counterion binding to the surface aggregates. It is important to obtain information about the layer thickness of the film adsorbed onto the graphite in order to be able to investigate the layer structure. As the tip approaches the sample, the short-range repulsive force appears in the force curve and then there is a point at which the tip moves into the substrate discontinuously (in other words there is mechanical instability at this position). This mechanical instability is considered to be due to the displacement or peeling off of the surfactant layer on graphite. The distance at

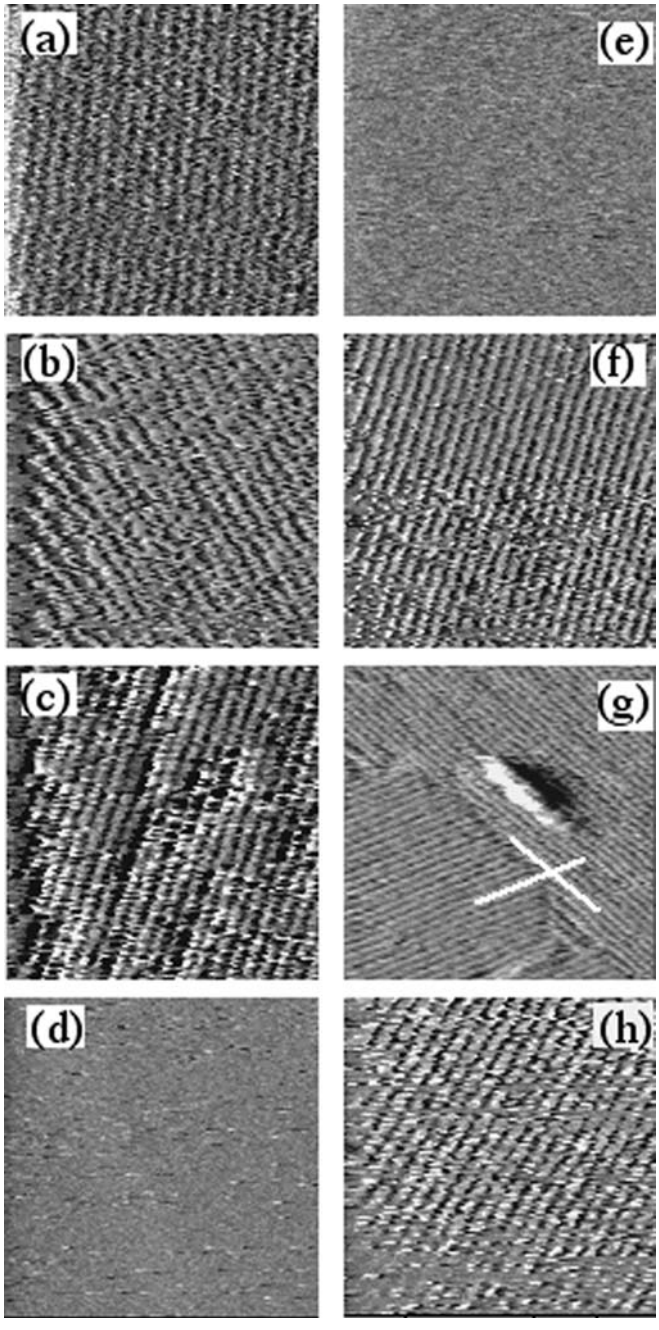

Fig. 2a–h AFM images showing the effect of the ionization on the aggregate structures of C12DMAO at the graphite-solution interface (100×100 nm^2). The surfactant concentration C_d was fixed to be about twice cmc. **a** $\alpha = 0.05$, pH 6 ± 0.2, $C_d = 3$ mM; **b** $\alpha = 0.15$, pH 5.5 ± 0.1, $C_d = 3$ mM; **c** $\alpha = 0.25$, pH 5 ± 0.1, $C_d = 5$ mM; **d** $\alpha = 0.37$, pH 4.5 ± 0.1, $C_d = 10$ mM; **e** $\alpha = 0.47$, pH 4.0 ± 0.1, $C_d = 10$ mM; **f** $\alpha = 0.55$, pH 3.7 ± 0.1, $C_d = 15$ mM; **g** $\alpha = 0.8$, pH 2.8 ± 0.1, $C_d = 15$ mM; **h** $\alpha = 0.9$, pH 2.3 ± 0.1, $C_d = 15$ mM. In (g), the 200×200 nm^2 AFM image shows the hemicylindrical aggregates oriented at 60° to each other (white lines)

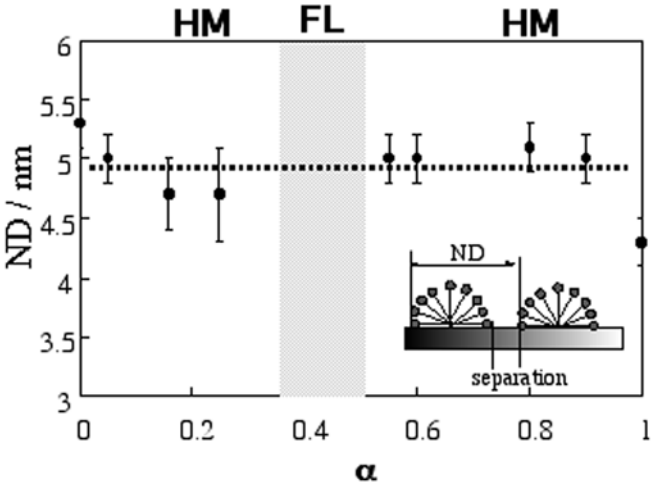

Fig. 3 Nearest-neighboring spacing (*ND*) of the hemicylindrical aggregates at the graphite-solution interface as a function of the degree of ionization α. HM: hemicylindrical aggregates; FL: laterally homogeneous layer

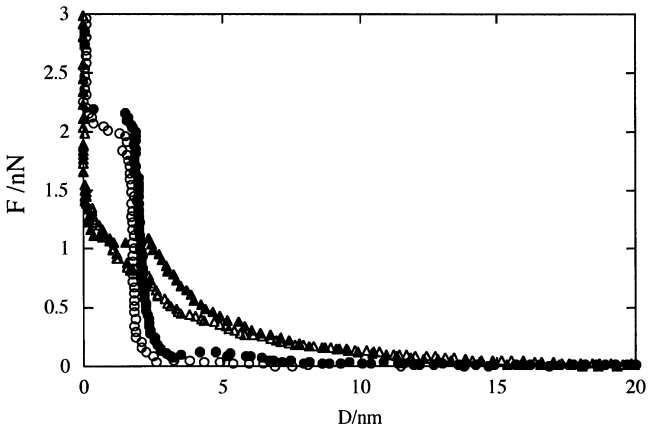

Fig. 4 Force between a silicon nitride tip and the graphite in the C12DMAO solution as a function of time for a pH jump of pH 8 (hemicylindrical aggregate) to pH 4 (laterally homogeneous layer). The force curves were obtained with the same tip and the same graphite, so that the relative magnitudes could be compared. Filled circles: pH 8 (before pH jump); unfilled triangles: 5 min after the injection of the HCI solution (pH jump from pH 8 to pH 4); filled triangles: 20 min after the injection of the HCI solution (pH jump from pH 8 to pH 4); unfilled circles: 20 min after the injection of the NaOH solution (pH jump from pH 4 to pH 8)

which the mechanical instability occurs in the force curve has been assigned to the adsorbed layer thickness between the tip and the substrate [9, 13, 33, 36]. In the case of C12DMAO aggregates on graphite, the distances at the mechanical instabilities occur are almost identical for the laterally homogeneous layer (2.1 ± 0.3 nm) and the half-cylindrical aggregate (1.9 ± 0.3 nm), as shown in Fig. 4, suggesting that the two adsorbed films on graphite have almost the same layer thickness. This in turn suggests that the laterally homogeneous layer has a monolayer structure. The observation of a long-range double-layer repulsive force in the force curve for the laterally homogeneous layer indicates that the cationic headgroups of the monolayer face the solution.

Reversible transformation between the laterally homogeneous layer and the hemicylindrical aggregate on graphite via changes in pH

Our results suggest a pH-induced transformation of the C12DMAO micellar aggregate between a hemicylindrical aggregate and the laterally homogeneous layer at the graphite-solution interface. The reversibility of the transformation between the hemicylindrical aggregate (pH 8, $\alpha = 0$) and the laterally homogeneous layer (pH 4, $\alpha \sim 0.5$) was also examined using force curves (Fig. 4) and AFM images (Fig. 5) in this study.

Hemicylindrical aggregate (pH 8) to laterally homogeneous layer (pH 4)

A sample was first equilibrated (for 24 h) and then the pH of the solution was changed by adding a small amount of HCl solution. At pH 8, before the injection of HCl solution, the C12DMAO forms hemicylindrical aggregates on graphite, as shown in Fig. 5a. In the corresponding force curve, there is no sign of a long-range repulsive force, but a short range repulsive force (< 3 nm) is observed (filled circles, Fig. 4). This indicates the existence of adsorbed surfactants of nonionic C12DMAO on graphite. The repulsive force may originate from the hydration or the protrusion force of the headgroups of the adsorbed surfactants on graphite. After the HCl solution was injected into the cell in order to change the pH of the solution from pH 8 to pH 4, the short-range repulsive barrier disappeared and a double-layer repulsive force was clearly observed after less than 5 min (unfilled triangles), suggesting that protonation of the adsorbed films on graphite occurs immediately after the injection. After about 20 min, the short-range repulsive barrier appeared again (filled triangles), but its value (about 1 nN) is smaller than that for $\alpha = 0$ before the pH jump (about 2 nN). This force curve after about 20 min was in good agreement with those after 60 min (not shown), suggesting the completion of the transformation from the hemicylinder to the laterally homogeneous layer. The observation of a featureless AFM image after about 25 min supports the formation of a laterally homogeneous layer (Fig. 5b).

Laterally homogeneous layer (pH 4) to hemicylindrical aggregate (pH 8)

Next we added NaOH solution into the cell in order to restore the pH of the solution from pH 4 to pH 8.

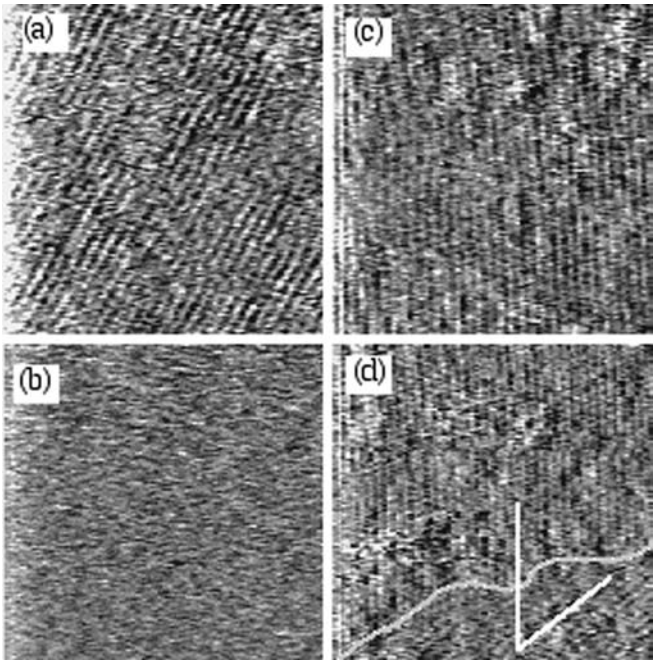

Fig. 5a–d AFM images (200×200 nm^2) of the aggregate structure of C12DMAO at the graphite-solution interface for a pH jump from pH 8 (hemicylindrical aggregate) to pH 4 (laterally homogeneous layer). The surfactant concentration was 15 mM. **a** pH 8 (before pH jump); **b** 25 min after the injection of the HCI solution (pH jump from pH 8 to pH 4); **c** 25 min after the injection of the NaOH solution (pH jump from pH 4 to pH 8); **d** 15 min after the injection of the NaOH solution (pH jump from pH 4 to pH 8). The AFM image (**d**) shows the hemicylindrical aggregates oriented at 50° to each other (white lines); the gray line represents the boundary. The AFM image in Figs. 5c,d were taken at the same sample position. The AFM images in Figs. 5a,b,c were taken at different sample positions, but we made sure that the whole sample was covered uniformly by one type of structure when capturing each of these AFM images

20 min after the injection of NaOH solution, the force of the repulsive barrier in the force curve (unfilled circles in Fig. 4, about 2 nN) recovered to almost the same as for $\alpha = 0$ before the pH jump (filled circles in Fig. 4, about 2 nN), and the double-layer repulsive force simultaneously disappeared. The AFM image after about 25 min indicates the formation of the hemicylindrical aggregate (Fig. 5c). This suggests the completion of the transformation from the laterally homogeneous layer to the hemicylinder.

The above results strongly suggest that the transformation between the hemicylindrical aggregate and the laterally homogeneous layer is reversible with respect to a pH change:

hemicylindrical aggregate (pH 8)
$\Leftrightarrow$ laterally homogeneous layer (pH 4)

By estimating the *ND* values obtained from the Fourier transforms of the two AFM images (Figs. 5a,c), and comparing them, we confirmed this reversible transformation of the micellar aggregates. If the formation of the hemicylindrical aggregates is truly reversible, they should be of comparable size. We found that the *ND* values obtained from the two AFM images were consistent with each other ($ND = 5.3 \pm 0.3$ nm from the AFM image of Fig. 5a, and $ND = 5.2 \pm 0.3$ nm from the AFM image of Fig. 5c), suggesting that the two hemicylindrical aggregates are in a comparable size. This provides further evidence for the reversible transformation between the hemicylindrical aggregate and the laterally homogeneous layer via a change in pH. It should be noted that the pH-induced transformation between the hemicylindrical aggregate and the laterally homogeneous layer may occur with a timescale $\ll$20 min, since it took about 10 min to equilibrate the pH after the injection of the NaOH solution or the HCl solution in this experiment.

It should also be added that the force curves depend on the solution medium (the ionic strength and the concentrations of the sodium cation or the chloride anion) as well as the layer structure on graphite. The ionic strength of the solution medium differed between the force curves at pH 8 (unfilled and filled circles in Fig. 4) due to the sodium chloride salt of 7.5 mM produced in the neutralization process. However, we consider that the sodium chloride salts produced have a minor effect on these force curves, since the C12DMAO layers consist of the nonionic surfactants at pH 8. The short-range repulsive barriers originated from the layer structure on graphite (the hydration or the protrusion force of the headgroups of the adsorbed surfactants on graphite) are considered to be almost independent of the produced salts. It may therefore be possible to use the short-range repulsive barrier of the force curves at pH 8 as one of the criterions for the restoration of the C12DMAO hemicylindrical aggregates.

In the kinetic process of the transformation from the laterally homogeneous layer to the hemicylinder (the pH jump of the solution from pH 4 to pH 8), we observed a region where the hemicylindrical aggregates occur in a different orientation to each other (Fig. 5d), but finally the oriented hemicylindrical aggregates disappeared and a single type of hemicylindrical structure covered the sample region uniformly (Fig. 5c).

It is not easy to interpret the observations made in this study. However, note that the hemicylindrical aggregates shown in Fig. 5d are oriented at about 50° to each other. This angle (shown by the white lines) is different to that of the equilibrium hemicylindrical aggregate on graphite, which occurs in only three orientations at 60° to each other [3, 4, 5, 9]. It has been suggested that the surfactant tail is oriented parallel to the three equivalent symmetry axes of the graphite basal plane in the horizontal adsorbed monolayer, resulting in

the formation of the hemicylindrical aggregate in three orientations at 60° to each other [3, 4, 5, 9]. Recent observations using a scanning tunneling microscope (STM) provide direct support for this model [37]. Similar hemicylindrical aggregates orientated at 60° were also observed for the equilibrium hemicylindrical aggregates of C12DMAO, as shown in Fig. 2g (white lines). The hemicylindrical aggregates oriented at about 50° might be metastable due to some kinetic mismatch between the flat-lying alkyl skeleton and the graphite lattice in the horizontal monolayer.

Formation of the laterally homogeneous layer at the graphite-solution interface in the C12DMAO surfactant system

In the C12DMAO aggregates on graphite, when the degree of ionization α was increased the following transition was observed: hemicylinder ($0 \leqq \alpha \leqq 0.25$), to the laterally homogeneous layer ($0.37 \leqq \alpha \leqq 0.47$), to hemicylinder ($0.55 \leqq \alpha \leqq 1$). These results indicate that the mean curvature of the surface aggregate of C12DMAO on graphite minimizes at $\alpha \sim 0.5$. To our knowledge, the only reported exception to the formation of hemicylindrical aggregates on graphite by ionic surfactants with tails longer than a decyl group occurs for the sodium dodecylsulfate-dodecanol system imaged at a graphite-solution interface [33], where the coexistence of hemicylinders with the laterally homogeneous layers was only observed below the cmc. From the viewpoint of the packing parameter argument of the surfactant [38], we would expect that the ionization of C12DMAO induces aggregates with a higher curvature due to the electrostatic repulsion between the headgroups. In the terms of the electrostatic repulsion between the headgroups only, therefore, the transformation from the hemicylindrical aggregate to the laterally homogeneous layer by charging up the aggregate cannot be understood. Some additional forces should exist in the half-ionized C12DMAO to overcome the free-energy barrier to the formation of the laterally homogeneous layers on graphite. There may be two possible contributions to the formation of the laterally homogeneous layer around $\alpha = 0.5$:

1. The laterally homogeneous layer on graphite is stabilized by the hydrogen bond between the cationic-nonionic headgroups (-N^+-OH··O-N-), as strongly suggested for the soluble monolayer of C12DMAO [24, 25] and the insoluble monolayer of C22DMAO [39] at the air/water interface. Spectroscopic evidence for the hydrogen bond between the headgroups on the cationic-nonionic pair has been also reported for the half-ionized C12DMAO in the lyotropic hexagonal phase and the micellar solution, as well as that in the solid state using a Fourier transform infrared spectrophotometer (FT-IR) [28, 40]. Due to the hydrogen bond between the headgroups, the area per headgroup decreases, leading to the higher packing parameter character of the aggregates on graphite for the half-ionized C12DMAO. The free energy of the hydrogen bond between the cationic-nonionic headgroups has been reported to be 2.3 kT for C12DMAO via hydrogen ion titration of the micelles in bulk solution [24, 25]. In the case of surfactants with twelve-hydrocarbons, it has been reported that there is a free energy difference of roughly 2–3 kT between the unfavorable vertical monolayer and the hemicylindrical aggregate at the hydrophobic solid-solution interface on the basis of thermodynamic modeling [17]. The free energy gain of the hydrogen bond may compensate for the free energy penalty of forming the unfavorable laterally homogeneous layer on graphite in the case of the half-ionized C12DMAO. As the electrostatic repulsion between the headgroups gets stronger as the ionization is increased beyond $\alpha = 0.5$, it is likely that the hydrogen bond contribution is overwhelmed by the increased electrostatic interaction, leading to the formation of the hemicylindrical aggregate with a higher curvature above $\alpha = 0.55$.
2. In the case of C12DMAO with $\alpha = 0.5$, there might be low ordering for the horizontal monolayer on graphite surface due to the mismatch between the pseudo-double-tailed surfactant of the C12DMAO by the hydrogen bonding and the graphite lattice, leading to disturbed formation of the hemicylindrical aggregates on graphite for C12DMAO around $\alpha = 0.5$. As for the hemicylindrical aggregates of the C12DMAO at $\alpha = 0$ and $\alpha = 1$, we sometimes observed parallel stripe structures even if the applied force is increased beyond the force at the mechanical instability, where the displacement of the surfactant aggregate occurs. The parallel stripe structures seen for force beyond the mechanical instability may correspond to the horizontal monolayer lying parallel to the graphite surface under the hemicylindrical aggregates [41, 42, 43]. For the laterally homogeneous layer of the C12DMAO around $\alpha = 0.5$, on the other hand, we have never observed the parallel stripe structures beyond the force at the mechanical instability, implying the disturbance of the horizontal monolayer on graphite. In our previous paper, we reported that all structures of C14DMAO on graphite were hemicylinders, irrespective of the ionization [31]. For the C14DMAO surfactant, the attractive interaction between the hydrocarbon chain and the graphite surface is stronger than that of the C12DMAO surfactant. As a result, the dominant attractive interaction between the tetradecyl group and the graphite surface may overcome the contribution from the hydrogen bonds between the headgroups of C14DMAO, in contrast to the case of C12DMAO.

Conclusions

The effect of ionization on the surface aggregate of dodecyldimethylamine oxide (C12DMAO) at the graphite-solution interface was investigated via atomic force microscopy (AFM). We have demonstrated the pH-induced transformation of the micellar aggregates on graphite between a hemicylinder and a laterally homogeneous layer. Nonionic C12DMAO and fully ionized cationic C12DMAO both formed hemicylindrical aggregates at graphite-solution interfaces, which are in good agreement with those observed for many other ionic (or nonionic) surfactants on graphite. For nearly half-ionized C12DMAO (a 1:1 mixture of the nonionic and the cationic species), however, the laterally homogeneous layer with monolayer structure was observed. The results indicate that the surface curvature of the C12DMAO aggregates on graphite is the lowest at a degree of ionization $\alpha \sim 0.5$. It is likely that the laterally homogeneous layer on graphite originates from the hydrogen bonding between the cationic-nonionic headgroups.

The pH-induced morphological transition takes place over a narrow range of pH: hemicylinder ($pH \geqq 5$), to laterally homogeneous layer ($4.5 \geqq pH \geqq 4$), to hemicylinder ($pH \leqq 3.7$). By interpreting AFM images and the force curves, the transformation between the hemicylindrical aggregate and the laterally homogeneous layer was found to be reversible with respect to a pH change.

During the kinetic process of the transformation from the laterally homogeneous layer to the hemicylinder (the pH jump of the solution from pH 4 to pH 8), we observed a region where the hemicylindrical aggregates are oriented at 50° to each other, which may indicate a metastable structure. This orientation angle was different from that of the equilibrium hemicylindrical aggregates, which were oriented at about 60° to each other.

Acknowledgements This work is supported, in part, by the Grant-in Aid for Scientific Research (No. 15750121) from The Monbukagaku-shou Japan, and in part by the Mitsubishi Chemical Corporation Fund. This study was partially supported by Industrial Technology Research Grant Program '03 from the New Energy and Industrial Technology Development Organization (NEDO) of Japan.

References

1. Gaudin AM, Fuerstenau DW (1955) T AIME 1
2. Gaudin AM, Fuerstenau DW (1955) T AIME 958
3. Manne S, Cleveland JP, Gaub HE, Stucky GD, Hansma PK (1994) Langmuir 10:4409
4. Manne S, Gaub HE (1995) Science 270:1480
5. Wanless EJ, Ducker WA (1996) J Phys Chem B 100:3207
6. Warr GG (2000) Curr Opin Colloid In 5:95
7. Tiberg F, Brinck J, Grant L (2000) Curr Opin Colloid In 4:411
8. Liu J-F, Ducker WA (1999) J Phys Chem B 103:8558
9. Wanless EJ, Ducker WA (1997) Langmuir 13:1463
10. FitzGerald PA, Warr GG (2001) Adv Mater 13:967
11. Lamont R, Ducker WA (1997) J Colloid Interf Sci 191:303
12. Grant LM, Tiberg F, Ducker WA (1998) J Phys Chem B 102:4288
13. Kiraly Z, Findenegg GH (1998) J Phys Chem B 102:1203
14. Grant LM, Edeth T, Tiberg F (2000) Langmuir 16:2285
15. Wolgemuth JL, Workman RK, Manne S (2000) Langmuir 16:3077
16. Bandyopadhyay S, Schelly JC, Tarek M, Moore PB, Klein ML (1998) J Phys Chem B 102:6318
17. Jonson RA, Nagarajan R (2000) Colloid Surface A 167:21
18. Herrmann KW (1962) J Phys Chem 66:295
19. Tokiwa F, Ohki K (1966) J Phys Chem 70:3437
20. Maeda H, Tsunoda M, Ikeda S (1974) J Phys Chem 78:1086
21. Ikeda S, Tsunoda M, Maeda H (1979) J Colloid Interf Sci 70:448
22. Warr GG, Grieser F, Evans DF (1986) J Chem Soc Farad T 1 82:1829
23. Rathman JF, Christian SD (1990) Langmuir 6:391
24. Maeda H (1996) Colloid Surface A 109:263
25. Maeda H, Kakehashi, R (2000) Adv Colloid Interfac 88:275
26. Kawasaki H, Fukuda T, Yamamoto A, Fukada K, Maeda H (2000) Colloid Surface A 169:117
27. Miyahara M, Kawasaki H, Fukuda T, Ozaki Y, Maeda H. (2001) Colloid Surface A 183–185:475
28. Kawasaki H, Maeda H (2001) Langmuir 17:2279
29. Kawasaki H, Ookuma K, Maeda H (2002) J Colloid Interf Sci 252:419
30. Kawasaki H, Souda M, Tanaka S, Nemoto N, Karlsson G, Almgren M, Maeda H (2002) J Phys Chem B 106:1524
31. Kawasaki H, Shutou M, Maeda H (2001) Langmuir 17:8210
32. Davey TW, Warr GG, Almgren M, Asakawa T (2001) Langmuir 17:5283
33. Maeda H, Kanakubo Y, Miyahara M, Kakehashi R, Garamus V, Pedersen JS (2000) J Phys Chem B 104:6174
34. Miyahara M, Kawasaki H, Garamus VM, Nemoto N, Kakehashi R, Tanaka S, Annaka M, Maeda H (2004) Colloid Surface B (submitted)
35. Ducker WA, Wanless EJ (1996) Langmuir 12:5915
36. Patrick HN, Warr GG, Manne S, Aksay IA (1999) Langmuir 15:1685
37. Xu SL, Wang C, Zeng, QD, Wu P, Wang ZG, Yan HK, Bai CL (2002) Langmuir 18:657
38. Israelachvili JN, Mitchel DJ, Ninham BW (1976) J Chem Soc Farad T 2 72:1525
39. Goddard ED, Kung HC (1973) J Colloid Interf Sci 43:511
40. Rathman JF, Scheuing DR (1990) ACS Sym Ser 447 7:123
41. Grant LM, Ducker WA (1997) J Phys Chem B 101:5337
42. Wanless EJ, Davey TW, Ducker WA (1997) Langmuir 13:4223
43. Holland NB, Ruegsegger M, Marchant RE (1998) Langmuir 14:2790